

12. PHYSICAL PROPERTIES ALONG THE DEVELOPING DÉCOLLEMENT IN THE NANKAI TROUGH: INFERENCES FROM 3-D SEISMIC REFLECTION DATA INVERSION AND LEG 190 AND 196 DRILLING DATA¹

Nathan L.B. Bangs² and Sean P.S. Gulick²

ABSTRACT

In the Nankai Trough, the décollement megathrust initiates within the incoming sedimentary sequence along an interface within the lower Shikoku Basin facies. Scientists on Ocean Drilling Program Legs 190 and 196 penetrated the stratigraphic horizon that develops into the décollement at a reference site 12 km seaward of the deformation front, Site 1173, and in the décollement zone, at Site 1174. The core and logging-while-drilling data collected at these sites examine the lateral variation in physical properties prior to and just after initiation of décollement thrusting. We used a prestack time migrated three-dimensional (3-D) seismic reflection data volume that overlaps with the Leg 190 and 196 drill sites, along with Site 1173 and Site 1174 physical property data, to invert a seismic reflection transect (Line 215) for seismic impedance across the trench from Site 1173 to the deformation front. We used porosity estimated from seismic inversion to infer compaction and dewatering activity within the upper and lower Shikoku Basin facies as the trench wedge overburden rapidly accumulates. A compacted layer (with porosity = ~40%) develops at the upper/lower Shikoku Basin facies boundary and the stratigraphic equivalent of the décollement zone in the trench landward of Site 1173. The compacted layer may develop because of localized dewatering, diagenetic, or cementation effects within the compacted layer or the over- and under-

¹Bangs, N.L.B., and Gulick, S.P.S., 2005. Physical properties along the developing décollement in the Nankai Trough: inferences from 3-D seismic reflection data inversion and Leg 190 and 196 drilling data. *In* Mikada, H., Moore, G.F., Taira, A., Becker, K., Moore, J.C., and Klaus, A. (Eds.), *Proc. ODP, Sci. Results*, 190/196, 1–18 [Online]. Available from World Wide Web: <<http://www-odp.tamu.edu/publications/190196SR/VOLUME/CHAPTERS/354.PDF>>. [Cited YYYY-MM-DD]

²Institute for Geophysics, University of Texas at Austin, 4412 Spicewood Springs Road, Austin TX 78759, USA. Correspondence author: nathan@ig.utexas.edu

lying layers. We speculate that the compacted layer serves as an aquitard to delay consolidation beneath the horizon that becomes the décollement zone and contributes to the décollement development.

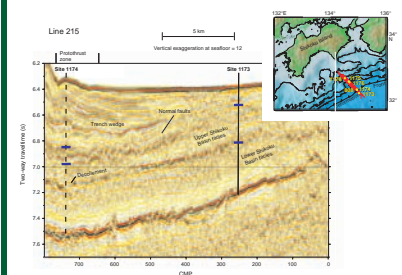
INTRODUCTION

Initiation of the décollement, or plate-boundary fault, plays a critical role in the structural and tectonic development of subduction zones. Décollement initiation partitions the trench stratigraphic section into an accreted section that grows the accretionary wedge and a subducted section that carries fluids and various chemical species deep into the subduction zone. These subducted sediments ultimately affect subduction zone geochemistry, thermal structure, and seismogenesis (e.g., Plank and Langmuir, 1993; Ruff and Kanamori, 1983). Understanding the initiation of the décollement is critical not only to understanding how faults initiate, but ultimately to understanding the controls on sediment flux either into the accretionary wedge or down the subduction zone.

Scientists on Ocean Drilling Program (ODP) Legs 131, 190, and 196 in the Nankai trough penetrated the décollement and the undeformed trench reference section and determined that the décollement initiates in the lower Shikoku Basin facies (Fig. F1), a nearly lithologically homogeneous hemipelagic mudstone (Mikada, Becker, Moore, Klaus, et al., 2002; Moore et al., 2001b; Taira, Hill, Firth, et al., 1991). The décollement also initiates beneath the rapidly deposited trench turbidite wedge. Whereas cementation may have a role in the development of the strength of the lower Shikoku Basin facies and influence décollement stratigraphic position due to the presence of authigenic clay minerals (Morgan and Ask, 2004), there are minimal physical property or lithologic changes that could be recognized as an inherent condition for a décollement at the trench reference site (Site 1173). This has prompted others to suggest that décollement initiation is a function of pore fluid pressures that develop following rapid loading within the low-permeability Shikoku Basin formation rather than a function of physical property conditions at a lithologic boundary (Le Pichon et al., 1993; Morgan and Karig, 1995; Screaton et al., 2002).

Screaton et al. (2002) hypothesize that overpressures develop beneath the décollement by comparing porosity of the underthrust section below the décollement to the reference site and suggest fluid pressures have a role in initiation of the décollement. However, the ways in which fluid pressures develop across the trench and lead to initiation and propagation of the décollement along a roughly consistent stratigraphic horizon are not well understood. In 1999, we acquired a large volume of three-dimensional (3-D) seismic reflection data across Leg 131 and the planned Leg 190 and 196 drill sites in an effort to image the décollement from the trench into the seismogenic zone. These data span the trench from the reference site to Sites 808 and 1174 and contain seismic velocity and impedance (velocity \times density) information that can provide a regional view of physical properties between the drill sites. The goal of this paper is to invert the 3-D seismic reflection data for seismic impedance and porosity with constraints from Leg 190 and 196 drilling data to infer the porosity and interpret subtle dewatering, consolidation, or diagenetic processes that contribute to form a weak horizon that becomes the décollement.

F1. Seismic Line 215, p. 13.



GEOLOGIC SETTING

The Nankai Trough is a sediment-filled trench common to convergent margins worldwide. It forms as the oceanic crust of the Philippine Sea plate subducts beneath the islands of Japan on the Eurasian plate at a modest rate of ~2–4 cm/yr (Seno et al., 1993) (Fig. F1). Along the Muroto Transect, the subducting crust is young (16 Ma) (Mikada, Becker, Moore, Klaus, et al., 2002), making the subducting crust relatively high temperature and shallow for a subduction zone trench. The trench floor lies at a water depth of ~4800 m, and ~1100 m of sediments compose the trench section in the prot thrust zone at the deformation front (Gulick et al., 2004; Moore et al., 2001a). Across the trench, the subducting crust dips at an angle of ~1° (Fig. F1).

Site 1173

During Legs 190 and 196, Site 1173 was drilled 12 km seaward of the accretionary wedge deformation front as a reference section to characterize the incoming stratigraphic sequence before deformation and to investigate the future décollement horizon physical properties prior to thrust initiation (Moore, Taira, Klaus, et al., 2001; Mikada, Becker, Moore, Klaus, et al., 2002). Drilling recovered a thin (102 m) sandy trench fill section of Quaternary sediment overlying the hemipelagic Shikoku Basin facies. At Site 1173, the upper Shikoku Basin facies is a 200-m-thick sequence of hemipelagic mud and claystone with interbedded ash layers. The lower Shikoku Basin facies is an almost 350-m-thick, Pliocene–middle Miocene sequence of lithologically homogeneous mud and claystone. The only significant lithology change within this section is in the proportion of clay minerals ~40 m beneath the upper/lower Shikoku Basin facies boundary, which is attributed to partial alteration of smectite to illite (Steurer and Underwood, this volume). There are also related microstructural changes with distinctive clay textures that may affect lithification (Sunderland and Morgan, this volume). From correlation of magnetic susceptibility signatures, the age equivalent sequence to the décollement zone drilled at Sites 1174 and 808 occurs between 40 and 70 m below the upper/lower Shikoku Basin facies boundary (390–420 mbsf) at Site 1173 (Moore et al., 2001b). In this paper we refer to this zone as the stratigraphic equivalent of the décollement zone. We note that Site 1173 is not on the same seismic line as Site 1174 but is offset on a parallel seismic line 3.25 km to the southwest. The stratigraphic equivalent of the décollement zone interpreted from the 3-D seismic data does not follow a consistent stratigraphic horizon parallel to the trench and appears to step down ~50 m from Site 1173 to Site 1174, introducing some uncertainty into the stratigraphic equivalent of the décollement zone at Site 1173.

One of the remarkable observations at Site 1173 is the large physical property change across the upper/lower Shikoku Basin facies boundary. Logging-while-drilling (LWD) and core density data show little vertical change in densities throughout the 240-m-thick upper Shikoku Basin facies, and these data deviate significantly from normal compaction trends (Moore et al., 2001b). In contrast, the lower Shikoku Basin facies has a decreasing trend attributed to normal compaction (Mikada, Becker, Moore, Klaus, et al., 2002). The upper Shikoku Basin facies is believed to be partially supported by a cement (Moore et al., 2001b), possibly silica cement (Mikada, Becker, Moore, Klaus, et al., 2002);

however, other cements (e.g., clay mineral cement) have not been ruled out. The large density increase at the upper/lower Shikoku Basin facies boundary is attributed to a density transition from anomalously low densities, and thus high porosities, of the upper Shikoku Basin facies to normal densities within the lower Shikoku Basin facies. The density transition across the upper/lower Shikoku Basin facies is thought to be caused in part by the diagenetic mineral transition of opal-A to opal-CT (Morgan and Ask, 2004) or opal-CT to quartz (Mikada, Becker, Moore, Klaus, et al., 2002) and associated compaction. The upper Shikoku Basin facies develops as an underconsolidated section with anomalously high porosity that is maintained by grain-to-grain support from the cement. Pressure and temperature conditions cause a phase transition and loss of cement with an associated porosity reduction at the upper/lower Shikoku Basin facies boundary. Significant for this paper is the large velocity and density reduction, which causes an impedance boundary and a prominent reflection in the seismic section. At Site 1173, the reflection is a compound reflection. On Line 215 (Fig. F1), there is large lateral variability in amplitude and waveform of this compound reflection, especially where it intersects Site 1173 (Fig. F1). Interestingly, the porosity reduction across the upper/lower Shikoku facies boundary is not coincident with the stratigraphic equivalent of the décollement zone at Site 1173, so it does not appear to be directly linked to décollement initiation. Whereas the lithologic distinction between the upper Shikoku Basin facies and the lower Shikoku Basin facies is based on the presence of ash layers (Moore, Taira, Klaus, et al., 2001), which can exist or not because of diagenesis or deposition, it is only the coincidental physical property changes that we can link to the seismic data. For this paper we interpret the upper/lower Shikoku Basin facies boundary across the trench section from the seismic reflection generated by the physical property boundary, consistent with observations at Site 1173.

Site 1174

Site 1174 penetrated the trench section in the protothrust zone of the accretionary wedge and penetrated the décollement. Figure F1 shows the projection of Site 1174 on seismic Line 215, which is located 13 km north of Site 1173. Significantly for this paper, the upper Shikoku Basin facies at Site 1174 is 65 m thinner than at Site 1173, and it is possible that the diagenetic boundary has migrated upsection between Sites 1173 and 1174. The porosity contrast across the upper/lower Shikoku facies boundary is minimal at Site 1174. Porosity data show a near-normal porosity-depth profile, indicating considerable consolidation of the upper Shikoku Basin facies between Site 1173 and Site 1174. At Site 1174 the décollement lies 125 m below the upper/lower Shikoku Basin facies boundary (at Site 1173 the stratigraphic equivalent of the décollement lies 40–70 m below the upper/lower Shikoku Basin facies boundary) and is characterized by an increase in porosity from ~30%–38% across the interface (Moore et al., 2001b; Mikada, Becker, Moore, Klaus, et al., 2002).

3-D SEISMIC DATA

We acquired 81 80-km-long lines using a single streamer on board the *Ewing* in the summer of 1999 (Bangs et al., 2004). The lines were spaced 100 m apart, and the data covered an 8-km × 80-km area from

the Nankai Trough across the seawardmost 70 km of the plate-boundary fault (Fig. F1). Seismic lines were navigated with a differential Global Positioning System (GPS) navigational system provided by Racal for determining ship's position, shot spacing, and tail buoy location. The seismic source was a tuned 70-L (4273 in³) air gun array with 14 guns of various sizes ranging from 1.3 to 10.5 L (80 to 640 in³). The receiver array was *Ewing's* Syntrac 6000-m streamer with 240 channels at 25-m spacing. Data were recorded at 2-ms sampling intervals for 9 s. Depth control was maintained with control birds every 300 m, and streamer position was determined from reconstructions based on 11 compasses spaced every 600 m and tail buoy differential GPS data, which were available for about one-third of the time.

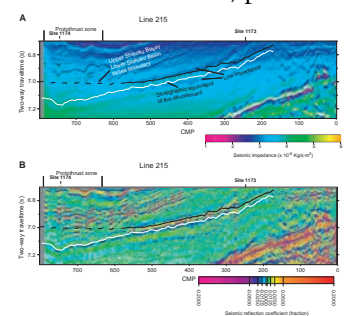
We constructed 3-D seismic images of the volume with 3-D prestack time migration. The data were binned at 50 m × 25 m and assigned source and receiver positions based on the differential GPS navigation. We produced the best images of the décollement when each of the ~34 million seismic traces was individually migrated in 3-D using a Kirchhoff prestack time migration algorithm with Paradigm's Geodepth software and migrated traces common to each bin were stacked to yield an image volume of 181 80-km-long lines with a cross-line spacing of 50 m. A portion of Line 215 across the trench and protothrust zone is displayed in Figure F1.

SEISMIC DATA INVERSION

The goal of the seismic inversion is to invert the prestack migrated profile Line 215 across the trench section, through Site 1173, for seismic impedance (velocity × density) to reveal the variation of physical properties at two key interfaces, the upper/lower Shikoku Basin facies boundary (black line, Fig. F2) and the stratigraphic equivalent to the décollement (white line, Fig. F2). The seismic inversion used a regularized least-squares algorithm based on Gauss-Newton optimization that was developed at the University of Texas Institute for Geophysics (Austin, Texas, USA) by Mrinal Sen and Indrajit Roy (Roy and Sen, 2001, 2002). The algorithm inverts the data trace by trace, seeking to minimize the residual error between a seismic impedance model convolved with an input source wavelet and the input data. The input data here are the Line 215 seismic traces extracted from the prestack migrated 3-D data volume. The source wavelet was extracted from the seafloor reflection in the undeformed, nearly flat-lying trench section.

The seismic inversion is excellent at deriving impedance contrasts across layered interfaces within the seismic reflection data, which reveals short-scale (tens of meters) variations of impedance; however, it is not able to determine the large-scale (hundreds of meters) vertical trends. For long wavelength variation in the seismic impedance we used Site 1173 wireline velocity and LWD density logs and Site 1174 core velocity and density data. Conversion of drilling data from depth to time was conducted using combined core and migration velocities, adjusting them to improve correlations between seismic reflections and seismic impedance from drilling data where possible. These data were smoothed with a 100-m-long running average to derive a long-wavelength profile. Relative impedance changes derived from seismic inversion were added to the long-wavelength impedance profile to obtain an absolute impedance profile with long and short wavelength variations. The analysis is inherently more sensitive to relative contrasts across in-

F2. Seismic impedance and seismic reflection coefficients, p. 14.



terfaces instead of absolute values, and the results are interpreted accordingly. The inversion results are shown in Figure F2.

Seismic impedance is difficult to use to infer lateral variations in physical properties directly related to compaction and dewatering processes, so estimates of seismic impedance were converted to porosity using an empirical relationship between impedance and porosity as described below. Seismic impedance is sensitive to porosity because it is the product of velocity and density, both of which vary with porosity in the same sense. It is unknown how cementation will bias porosity estimates from impedance. Figure F3 is a plot of the seismic impedance vs. porosity for upper and lower Shikoku Basin facies sediment as estimated from wireline logging velocities, LWD density, and core porosity. The small deviation above the fitted curve for samples with porosities between 50% and 60% in Figure F3 may be an effect of cementation. If so, effects are minimal. For our purposes, we assume porosity is the primary influence on impedance and cementation effects are secondary. This is discussed further below. We estimated an empirical relationship from the impedance vs. porosity data by fitting an exponential curve similar to the method used by Erickson and Jarrard (1999) for velocity/porosity relationships. The seismic impedance was converted to porosity with the empirical relationship, and the results are shown in Figure F4.

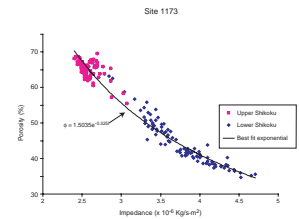
RESULTS

The upper/lower Shikoku Basin facies boundary and the stratigraphic equivalent to the décollement appear as two distinctive interfaces beneath the trench wedge in the inversion results (Fig. F2). The scale chosen to display the seismic reflection coefficients exaggerates the low values and emphasizes the distinctively separate interfaces. For the upper interface, the upper/lower Shikoku Basin facies boundary reflection coefficient increases by more than a factor of 2 from Site 1173 to the interval between common midpoints (CMPs) 350 and 550, indicating an increasing contrast above and below the upper/lower Shikoku Basin facies boundary. Landward of CMP 550 the upper/lower Shikoku Basin facies boundary seismic impedance and reflection coefficients show the contrast across this interface is virtually eliminated.

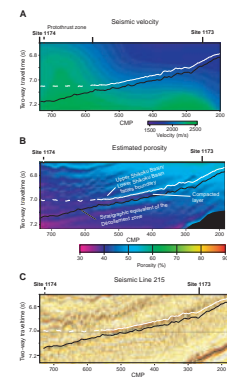
For the lower interface, the stratigraphic equivalent of the décollement, the reflection appears beneath the upper/lower Shikoku Basin facies boundary reflection between CMPs 350 and 550 (Fig. F2). It has a weak negative reflection coefficient that is not seen near Site 1173. The spacing between the upper/lower Shikoku Basin facies boundary and the stratigraphic equivalent to the décollement is close to seismic wavelengths of ~50 m, and the relatively high strength contrast of the upper/lower Shikoku Basin facies boundary makes it difficult to recognize the stratigraphic equivalent to the décollement interface in the original data. The inversion results help to show the existence of this weak reflection. The impedance contrast across this interface increases toward the protothrust zone, and thus the reflection coefficient decreases from approximately -.0125 to approximately -.025.

The separate interfaces at the upper/lower Shikoku Basin facies boundary and the stratigraphic equivalent to the décollement zone are much more apparent in a trench profile 2650 m farther to the northeast (Line 268) (Fig. F5). The décollement position shifts stratigraphically (Adamson et al., 2003) and forms deeper in the section to the northeast.

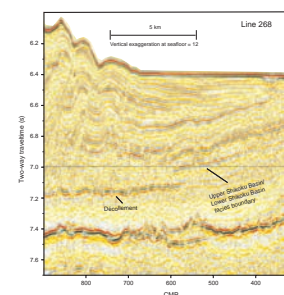
F3. Impedance vs. porosity, p. 15.



F4. Seismic velocity data and estimated porosity, p. 16.



F5. Trench section of Seismic Line 268, p. 17.



The vertical separation between the stratigraphic equivalent to the décollement and the upper/lower Shikoku Basin facies boundary is therefore greater along Line 268 than along Line 215. Figure F5 shows a clear example of the brightening of the upper/lower Shikoku Basin facies boundary reflection landward to its abrupt termination at CMP 600 as well as the underlying development of the stratigraphic equivalent to the décollement in the landward direction.

The conversion of impedance to porosity (Fig. F4) reveals lateral porosity variations that suggest how porosity evolved within these sediments to produce the seismic reflections along Line 215. Inversion of impedance associated with the high amplitude positive polarity reflection is consistent with an underconsolidated upper Shikoku Basin facies from Site 1173 to CMP 530. Porosity in this interval appears to change little in the landward direction despite the ~180 m of additional overburden. It is interesting to note the presence of a series of vertical fractures spaced ~250 m apart at approximately CMP 500 (Fig. F1). This series appears limited to the upper Shikoku Basin facies, consistent with the interpretation of Heffernan et al. (2004) that they are layer-bound compaction-related normal faults that potentially indicate fluid overpressuring. The large lateral porosity decline between CMPs 500 and 650 is consistent with an observed increase in seismic *P*-wave velocities from ~2.0 to ~2.4 km/s derived from velocity analysis for the prestack time migration of the same section (Fig. F4).

Beneath the upper/lower Shikoku Basin facies boundary and above the stratigraphic equivalent to the décollement, a layer of relatively low porosities develops near CMP 350 (between the black and white lines, Fig. F4) and extends toward the protothrust zone. Porosity within this layer is ~50% at Site 1173, but between CMPs 350 and 550 it reduces to ~40%. The lower Shikoku Basin facies sediments usually follow a normal compaction trend at Site 1173 (Morgan and Ask, 2004). The 40% porosity layer may simply be a normally consolidated layer, but the overlying upper Shikoku Basin facies and the lower Shikoku Basin facies just beneath the layer may be underconsolidated due to delayed consolidation and thus produce what appears to be a more compacted layer (Fig. F4).

DISCUSSION

The results from seismic inversion suggest dewatering and compaction or diagenesis and cementation activities in the trench sediment affect the development of a weak horizon seaward of the deformation front, as suggested by others (e.g., Shi and Wang, 1985, 1988; Le Pichon et al., 1993; Morgan and Karig, 1995; Morgan and Ask, 2004). At Nankai, the upper Shikoku Basin facies is critical to the compaction and dewatering of the trench sediment section because it has high porosity and potentially high permeability prior to accumulation of the trench wedge. It also appears to undergo substantial compaction in the trench (Moore, Taira, Klaus, et al., 2001). Consequently, the upper Shikoku Basin facies releases a large volume of fluids, which may induce hydrofracturing as indicated by vertical faults (Fig. F1) (Heffernan et al., 2004), and probably undergoes a substantial reduction in intergranular permeability from Site 1173 to the protothrust zone.

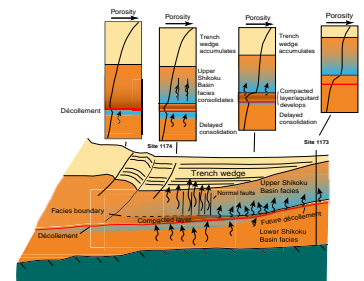
Our results suggest that consolidation of the upper Shikoku Basin facies has probably differed substantially from that of the lower Shikoku Basin facies, and the resulting permeability of the upper Shikoku Basin

facies has had a significant impact on consolidation of the lower Shikoku Basin facies. If we assume that lateral changes in porosity variations from Site 1173 to the deformation front reflect a time progression, we can interpret the evolution of porosity along the stratigraphic equivalent of the décollement. We observe a lateral increase in seismic impedance contrast across the upper/lower Shikoku Basin facies boundary between Sites 1173 and CMP 550 (Fig. F2). Vertical loading from progressive burial between Site 1173 and CMP 550 causes consolidation that increases the amplitude of the upper/lower Shikoku Basin facies boundary reflection. An increase in the seismic impedance beneath the upper/lower Shikoku Basin facies boundary is more likely than a decrease in impedance above the interface because the latter would require an unlikely porosity increase in the upper Shikoku Basin facies. Therefore, between CMPs 320 and 550, consolidation appears to preferentially reduce porosity within the uppermost lower Shikoku Basin sequence, between the upper/lower Shikoku Basin facies boundary and the stratigraphic equivalent of the décollement zone as indicated by the estimated porosity (Fig. F4).

We speculate that as the trench wedge accumulates the added overburden does not initially consolidate the high-porosity upper Shikoku Basin facies significantly. If the upper Shikoku Basin facies had consolidated across this interval it would have raised impedance, lessened the contrast with the underlying section, and produced a weaker seismic reflection. Therefore, the upper Shikoku Basin facies probably sustains little porosity change between Site 1173 and CMP 550. If we assume that intrinsic permeability varies systematically with porosity for these sediments (Saffer and Bekins, 1998), upper Shikoku Basin sediments will have a higher permeability than the underlying lower Shikoku Basin facies. The relatively high permeability of the underconsolidated upper Shikoku Basin facies may be a critical factor in maintaining near normal consolidation of the lower Shikoku Basin facies with progressive burial, but it may also contribute to preferentially consolidate the uppermost tens of meters of the lower Shikoku Basin facies as the initial response to burial by the trench wedge as predicted in the models of Le Pichon et al. (1993). If this interpretation is correct, then delayed consolidation may be a typical response to progressive burial except between the upper/lower Shikoku Basin facies boundary and the stratigraphic equivalent of the décollement zone as depicted by the cartoon in Figure F6. This model is similar to the model of Le Pichon et al. (1993), in which a high-permeability sandy layer rapidly deposited on top of low-permeability clays focuses consolidation at the top of the clay layer. The difference here is that a permeability contrast is presumed to exist between the upper and lower Shikoku Basin facies, and it initially focuses consolidation below this interface and forms a temporary, relatively low porosity layer at the top of the lower Shikoku Basin facies. It is this relatively low porosity layer that may serve as an aquitard to resist the upward migration of fluid from the lower Shikoku Basin facies and delay consolidation.

The compacted layer may also develop from the compactive deformation involving destruction of a porous cemented microfabric (Morgan and Ask, 2004; Ujiie et al., 2003). Microstructural studies by Ujiie et al. (2003) observed cementation due to intergranular bonding of authigenic clays in samples from Site 1173 taken from the stratigraphic equivalent of the décollement. In the equivalent samples at Site 1174, these sediments sustained an initial compactive deformation related to mechanical rather than chemical destruction of cementation. Ujiie et

F6. Schematic model of consolidation, p. 18.



al. (2003) also noted that cementation was also present within the décollement at Site 1174 but was much weaker or absent below it. If authigenic clay cementation is abundant above the stratigraphic equivalent of the décollement zone, its destruction either chemically or mechanically may account for the development of the compacted layer.

Morgan and Ask (2004) found evidence for clay mineral cementation beneath the stratigraphic equivalent of the décollement zone at Site 1173. They attribute the cementation to the growth of authigenic clay minerals following the alteration from smectite to illite. However, unlike the upper Shikoku Basin facies, which developed a cement prior to significant burial, possibly a silica cement, cementation in the lower Shikoku Basin section is a clay mineral cement that developed beneath the smectite/illite alteration boundary after substantial consolidation (Morgan and Ask, 2004). If the upper Shikoku Basin facies is supported in part by cement and the lower Shikoku Basin facies below the stratigraphic equivalent of the décollement zone is supported partially by an authigenic clay mineral cement, then the interval in between these cemented zones may be the only interval that can compact and maintain normal consolidation with accumulating overburden. The lateral development of the compacted zone between Sites 1173 and CMP 550 on Line 215 that we interpret from the seismic impedance inversion may be the result of dewatering and consolidation within this uncemented interval to a greater degree than the cemented intervals above and below it. It remains uncertain whether the presence of clay mineral cementation above and below the compacted layer is consistent with the observed increase and decrease in seismic impedance at the top and base of this layer, respectively. Cementation usually increases seismic velocities as observed from Site 1173 core samples from the upper Shikoku Basin section (Moore et al., 2001b). A decrease in seismic velocity that might be caused by loss of cement across the top of the compacted layer would also require a particularly large increase in density to compensate for the velocity and produce the observed seismic impedance. The reverse is true at the base of the compacted layer. For this reason we favor consolidation and dewatering mechanisms over cementation or diagenetic effects; however, it probably cannot be completely resolved with our data. In either case, there appears to be a compacted layer that could serve as an aquitard to restrict dewatering below the stratigraphic equivalent of the décollement zone.

Below the stratigraphic equivalent of the décollement zone porosity remains relatively high. As illustrated in Figure F4, a weak reflection at the stratigraphic equivalent of the décollement zone may initially develop from the contrast at the base of the compacted layer. It is this developing interface that can be traced continuously to the décollement. Figure F6 illustrates the possibility that the décollement simply forms at the base of the compacted layer.

Between CMPs 500 and 600 the upper Shikoku Basin facies consolidates substantially, as indicated by the velocity and porosity estimates in Figure F4. We interpret the decline in upper/lower Shikoku Basin facies boundary reflection between CMPs 500 and 600 as a result of consolidation of the upper Shikoku Basin facies. The closely spaced normal faults observed here extend through upper Shikoku Basin facies but not into the overlying or underlying sequences (Fig. F1). Heffernan et al. (2004) interpreted these faults as possible compaction structures. Coincident with the sharp decline in the impedance contrast of the upper/lower Shikoku Basin facies boundary at CMP 550 is the increase in amplitude of the stratigraphic equivalent of the décollement zone at

approximately CMP 600. Consolidation of the upper Shikoku Basin facies likely lowers its permeability further and restricts fluid flow and consolidation from beneath the stratigraphic equivalent of the décollement zone, contributing to the overpressured conditions as depicted in Figure F6. The development of a weak overpressured, underconsolidated décollement may ultimately be the result of differences in dewatering between the upper and lower Shikoku Basin facies as they respond to the rapidly accumulating overburden and undergo diagenesis. The position of the décollement may ultimately be a function of how thick the low-porosity layer becomes below the upper/lower Shikoku Basin facies boundary before décollement initiation. Similar examination of other transects both along the Muroto Transect (e.g., Line 268) and other transects (e.g. the Ashizuri Transect) (Moore, Taira, Klaus, et al., 2001) are necessary for further testing and development of this speculative model.

CONCLUSIONS

Inversion of the 3-D seismic reflection profile Line 215 through Site 1173 produced a model of porosity that illustrates details of the stratigraphic equivalent of the décollement zone as it evolves in the trench section seaward of the accretionary wedge (Fig. F6). As the trench wedge accumulates on top of the upper Shikoku Basin facies just landward of Site 1173, consolidation is focused at the top of the lower Shikoku Basin facies and a compacted layer develops between the upper/lower Shikoku Basin facies boundary and the stratigraphic equivalent of the décollement zone. We speculate that the compacted layer acts, at least temporarily, as an aquitard that delays consolidation beneath the compacted layer. Cementation both above and below the compacted layer could also restrict consolidation except within the compacted layer. It is within this section, at the base of the compacted layer, that the décollement initiates. If the compacted layer is unrelated to cementation, the thickness of the compacted layer probably varies with the permeability contrast between the lower Shikoku Basin and upper Shikoku Basin facies and other local dewatering effects. The extent to which this layer develops may determine the stratigraphic position of the décollement, which appears to deepen parallel to the deformation front from the transect at Site 1173 to the transect at Site 1174.

ACKNOWLEDGMENTS

We thank Indrigit Roy for the use of his seismic inversion algorithm and his efforts to implement it on our data. We thank Julia Morgan and an anonymous reviewer for thoughtful and detailed comments that helped this manuscript significantly. This research used samples and/or data provided by the Ocean Drilling Program (ODP). ODP is sponsored by the U.S. National Science Foundation (NSF) and participating countries under management of the Joint Oceanographic Institutions (JOI) Inc. This work was supported by NSF grant number OCE-9730637 and the United States Science Support Program. This manuscript represents UTIG contribution number 1692.

REFERENCES

- Adamson, S., Moore, J.C., Bangs, N.L., Gulick, S., and Moore, G.F., 2003. Controls on the morphological variability of the décollement in the Nankai Trough subduction zone. *Eos, Trans. Am. Geophys. Union*, 82 (Suppl.):T52B-0273. (Abstract)
- Bangs, N.L., Shipley, T.H., Gulick, S.P.S., Moore, G.F., Kuromoto, S., and Nakamura, Y., 2004. Evolution of the Nankai Trough décollement from the trench into the seismogenic zone: inferences from three-dimensional seismic reflection imaging. *Geology*, 32:273–276.
- Erickson, S.N., and Jarrard, R., 1999. Porosity-formation factor and porosity-velocity relationships in the Barbados prism. *J. Geophys. Res.*, 104:15391–15408.
- Gulick, S.P.S., Bangs, N.L.B., Shipley, T.H., Nakamura, Y., Moore, G., and Kuramoto, S., 2004. Three-dimensional architecture of the Nankai accretionary prism's imbricate thrust zone off Cape Muroto, Japan: prism reconstruction via en echelon thrust propagation. *J. Geophys. Res.*, 109:10.1029/2003JB002654.
- Heffernan, A.S., Moore, J.C., Bangs, N.L., Moore, G.F., and Shipley, T.H., 2004. Initial deformation in a subduction thrust system: polygonal normal faulting in the incoming sedimentary sequence of the Nankai subduction zone, southwestern Japan, application to the exploration of sedimentary basins. In Davies, R.J., et al. (Eds.), *3D Seismic Technology: Application to the Exploration of Sedimentary Basin*. Mem.—Geol. Soc. London, 29:143–148.
- LePichon, X., Henry, P., and Lallemand, S., 1993. Accretion and erosion in subduction zones: the role of fluids. *Annu. Rev. Earth Planet. Sci.*, 21:308–331.
- Mikada, H., Becker, K., Moore, J.C., Klaus, A., et al., 2002. *Proc. ODP, Init. Repts.*, 196 [CD-ROM]. Available from: Ocean Drilling Program, Texas A&M University, College Station TX 77845-9547, USA.
- Moore, G.F., Taira, A., Bangs, N.L., Kuramoto, S., Shipley, T.H., Alex, C.M., Gulick, S.S., Hills, D.J., Ike, T., Ito, S., Leslie, S.C., McCutcheon, A.J., Mochizuki, K., Morita, S., Nakamura, Y., Park, J.O., Taylor, B.L., Toyama, G., Yagi, H., and Zhao, Z., 2001a. Data report: Structural setting of the Leg 190 Muroto Transect. In Moore, G.F., Taira, A., Klaus, A., et al., *Proc. ODP, Init. Repts.*, 190, 1–14 [CD-ROM]. Available from: Ocean Drilling Program, Texas A&M University, College Station TX 77845-9547, USA.
- Moore, G.F., Taira, A., Klaus, A., et al., 2001. *Proc. ODP, Init. Repts.*, 190 [CD-ROM]. Available from: Ocean Drilling Program, Texas A&M University, College Station TX 77845-9547, USA.
- Moore, G.F., Taira, A., Klaus, A., and Leg 190 Scientific Party, 2001b. New insights into deformation and fluid flow processes in the Nankai Trough accretionary prism: results of Ocean Drilling Program Leg 190. *Geochem., Geophys., Geosyst.*, 2:10.1029/2001GC000166.
- Morgan, J.K., and Ask, M.V.S., 2004. Consolidation state and strength of underthrust sediments and evolution of the décollement at the Nankai accretionary margin: results of uniaxial reconsolidation experiments. *J. Geophys. Res.*, 109:10.1029/2002JB002335.
- Morgan, J.K., and Karig, D.E., 1995. Décollement processes at the Nankai accretionary margin, southeast Japan. *J. Geophys. Res.*, 100:15221–15231.
- Plank, T., and Langmuir, C.H., 1993. Tracing trace elements from sediment input to volcanic output at subduction zones. *Nature*, 362:739–743.
- Roy, I.G., and Sen, M.K., 2001. Robust waveform inversion by adaptive regularization. *Eos, Trans. Am. Geophys. Union*, 82 (Suppl.):S32C-0657. (Abstract)
- Roy, I.G., and Sen, M.K., 2002. Regularization methods in pre-stack waveform inversion. *Eos, Trans. Am. Geophys. Union*, 83 (Suppl.):S61B-1145. (Abstract)
- Ruff, L., and Kanamori, H., 1983. Seismic coupling and uncoupling at subduction zones. *Tectonophysics*, 99:99–117.

- Saffer, D.M., and Bekins, B.A., 1998. Episodic fluid flow in the Nankai accretionary complex: timescale, geochemistry, flow rates, and fluid budget. *J. Geophys. Res.*, 103:30351–30371.
- Screaton, E., Saffer, D., Henry, P., Hunze, S., and Leg 190 Shipboard Scientific Party, 2002. Porosity loss within the underthrust sediments of the Nankai accretionary complex: implications for overpressures. *Geology*, 30:19–22.
- Seno, T., Stein, S., and Gripp, A.E., 1993. A model for the motion of the Philippine Sea plate consistent with NUVEL-1 and geological data. *J. Geophys. Res.*, 98:17941–17948.
- Shi, Y., and Wang, C.-Y., 1985. High pore pressure generation in sediments in front of the Barbados Ridge Complex. *Geophys. Res. Lett.*, 12:773–776.
- Shi, Y., and Wang, C.-Y., 1988. Pore pressure generation in sedimentary basins: overloading versus aquathermal. *J. Geophys. Res.*, 91:2153–2162.
- Taira, A., Hill, I., Firth, J.V., et al., 1991. *Proc. ODP, Init. Repts.*, 131: College Station, TX (Ocean Drilling Program).
- Ujiie, K., Hisamitsu, T., and Taira, A., 2003. Deformation and fluid pressure variation during initiation and evolution of the plate boundary décollement zone in the Nankai accretionary prism. *J. Geophys. Res.*, 108:10.1029/2002JB002314.

Figure F1. Seismic Line 215 (displayed with high vertical exaggeration) shows the seismic stratigraphy along a transect perpendicular to the deformation front and intersecting Site 1173. The projection of Site 1174, located 3300 m to the northeast, is shown as a dashed line. (Inset) Location map shows the Muroto transect 3-D seismic data volume and ODP Leg 190 and 196 drill sites offshore Shikoku Island, southwest Japan. CMP = common midpoint.

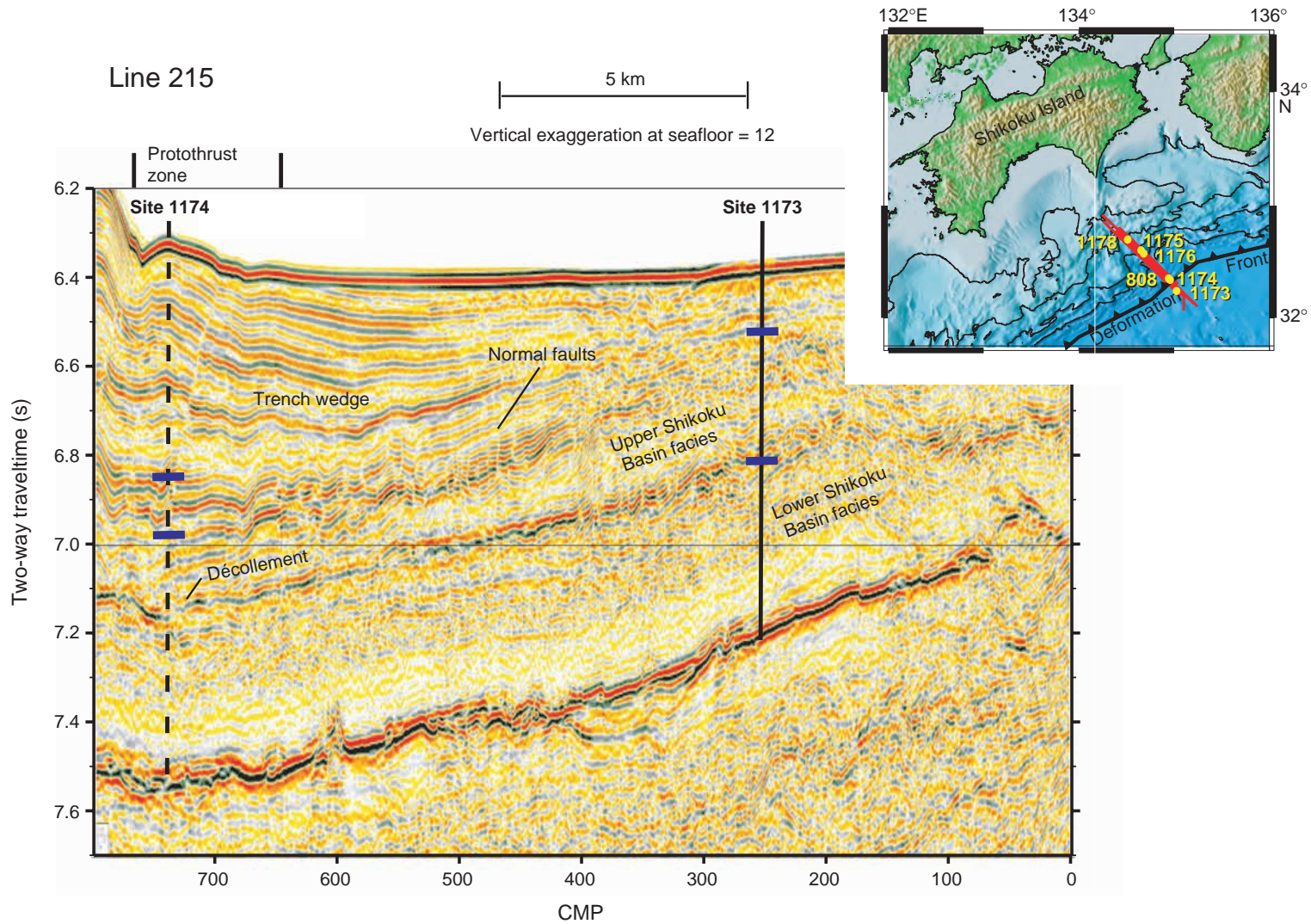


Figure F2. A. Seismic impedance derived from seismic inversion. Section shown is the section of interest around the upper/lower Shikoku Basin facies boundary (black line) and the stratigraphic equivalent of the décollement zone (white line) from Site 1173 to the deformation front. B. Seismic reflection coefficients also derived from the inversion across the same section as (A). Note the large color scale change at low coefficient values to emphasize the weak reflections. Reflection coefficients show more clearly that the two reflections, marked by the black and white lines, are separate. CMP = common midpoint.

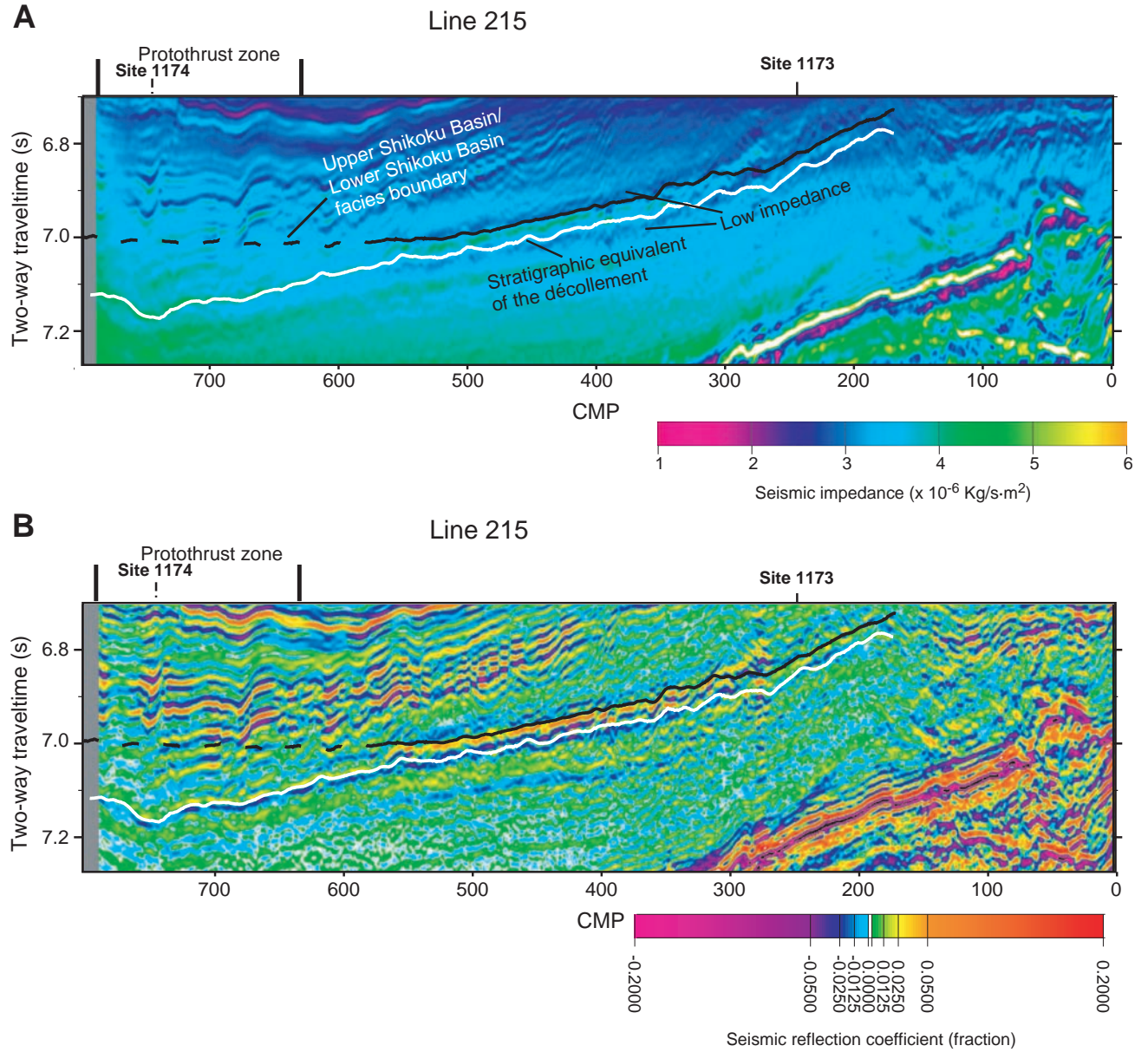


Figure F3. Impedance vs. porosity for upper and lower Shikoku Basin facies measured from Site 1173 core data and wireline logs. These data were fitted with an exponential curve as shown with ϕ = porosity and I = impedance. These results were used to estimate porosity from seismic impedance derived from the inversion as shown in Figure F4, p. 16.

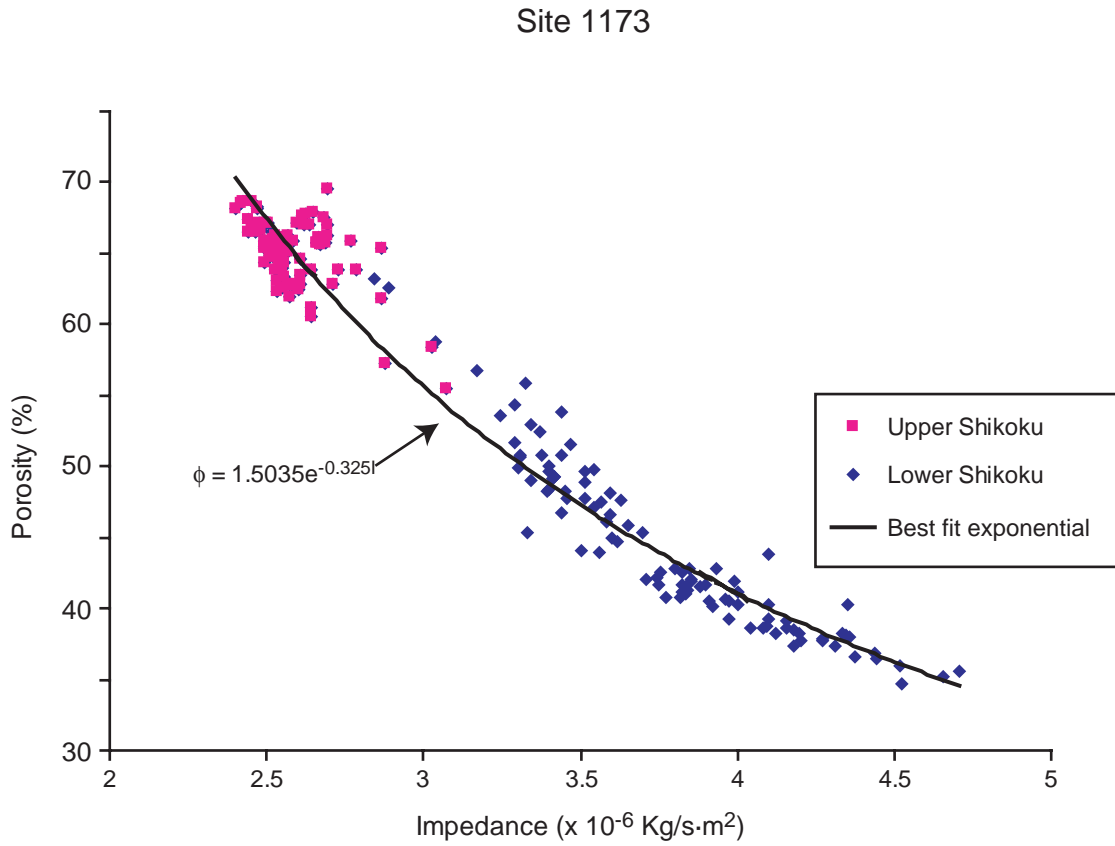


Figure F4. A. Seismic velocity data derived from velocity analysis for prestack time migration. These data were used with ODP Leg 190 and 196 core and log velocity and density data to constrain large-scale impedance variations in the impedance inversion. B. Estimated porosity derived from seismic impedance (Fig. F2, p. 14) and the empirical porosity/seismic impedance relationship (Fig. F3, p. 15). A significant, compacted layer between the upper/lower Shikoku Basin facies boundary and the stratigraphic equivalent of the décollement zone develops midway between Site 1173 and the deformation front. C. Seismic section equivalent to sections A and B. CMP = common midpoint.

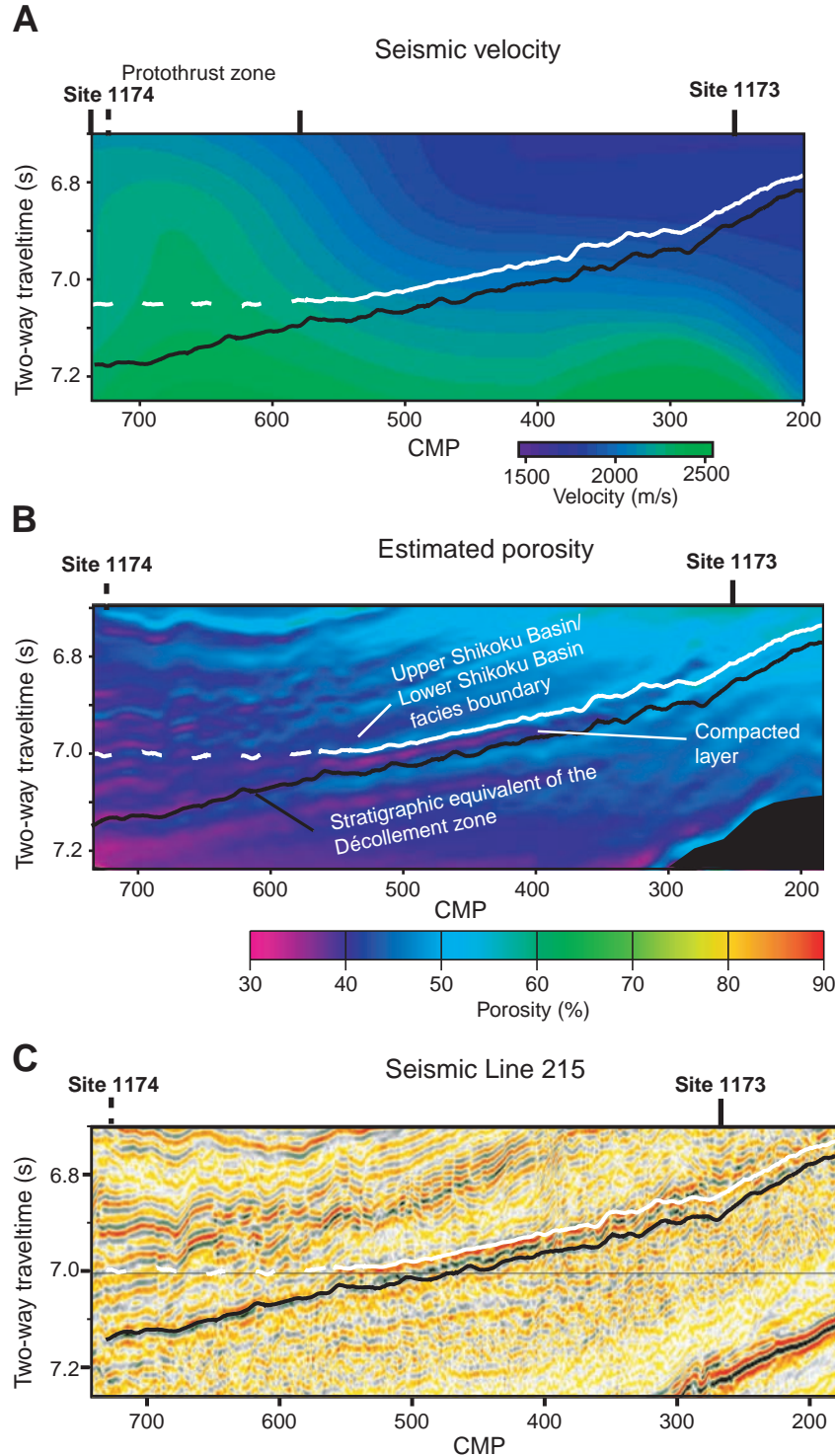


Figure F5. The trench section of seismic Line 268. This section shows clearly the lateral brightening of the upper/lower Shikoku Basin facies boundary reflection between common midpoints (CMPs) 400 and 600, and then its termination at CMP 600. The stratigraphic equivalent of the décollement zone is deeper here than on Line 215, making it easier to identify a layer between the upper/lower Shikoku Basin facies boundary and the stratigraphic equivalent of the décollement zone.

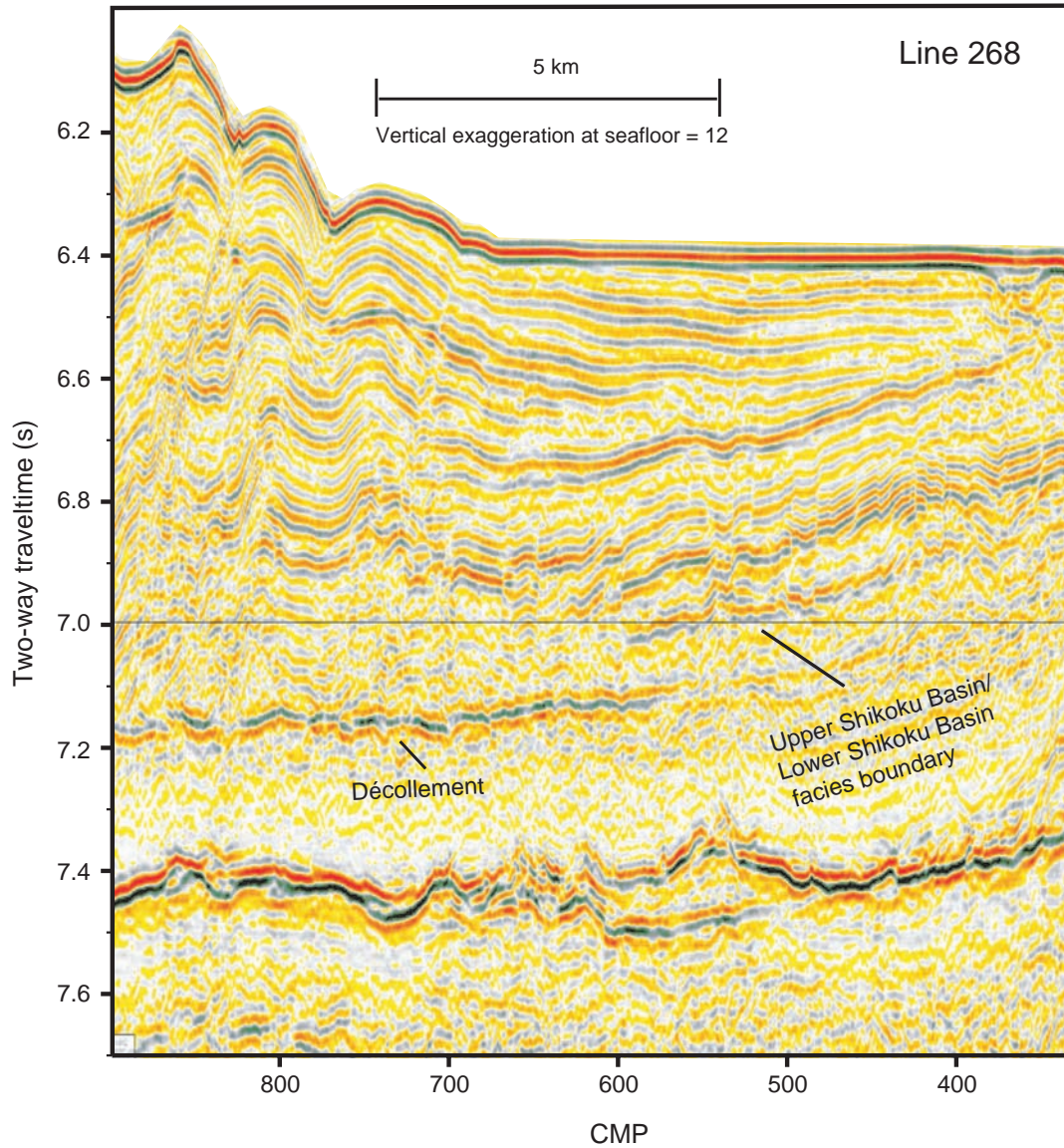


Figure F6. A schematic model of consolidation in the upper and lower Shikoku Basin facies across the trench. Blue sections represent underconsolidated sediment with relatively high permeability. Dark brown represents the compacted layer that develops between the upper/lower Shikoku Basin facies boundary and the stratigraphic equivalent of the décollement zone. Arrow represents focused fluid flow. Initial trench wedge accumulation causes a compacted layer (with presumed low relative permeability) to form in the top of the lower Shikoku Basin facies as fluids are expelled and are able to move through the underconsolidated upper Shikoku Basin facies. Compaction and fluid expulsion from the upper Shikoku Basin facies midway between Site 1173 and the deformation front causes an overpressured décollement zone to develop below the compacted layer.

